Chapter 6

The Effects of Lanthanum Dopant on the Structural and Optical Properties of Ferroelectric Thin Films

Irzaman, Hendradi Hardhienata,
Akhiruddin Maddu, Aminullah and Husin Alatas

Additional information is available at the end of the chapter

http://dx.doi.org/10.5772/intechopen.69029

Abstract

This chapter presents the effect of lanthanum (La) dopant on the structural and optical properties of the following ferroelectric thin films: barium strontium titanate ($Ba_{0.5}Sr_{0.5}TiO_3$) (BST), lithium tantalate ($LiTaO_3$), and lithium niobate ($LiNbO_3$). We applied X-ray diffraction, Fourier transform infrared spectroscopy (FTIR), and in some cases, atomic force microscopy to investigate the structural properties, functional groups, and particle size, as well surface roughness of these lanthanum-doped thin films, respectively, whereas ultra violet-visible (UV-Bis) spectrometer was applied to investigate the optical bandgap of the La-doped thin films. The results are in agreement with other previously researcher studies using different substrate materials. In general, the effect of La dopant highly affects both the structural and optical properties, changing significantly the grain size, surface roughness, and energy gap, and in certain cases, such as BST doped by La can change the material electric properties from insulator to semiconductor. Therefore, La-doped thin films may offer promising applications in the future.

Keywords: lanthanum dopant, optical properties, structural properties, thin films

1. Introduction

It is well known that lanthanum—denoted by the symbol La and atomic number 57—is one of the most abundant rare earth elements with the physical characteristics of being silvery white metallic. Lanthanum can be found in some rare-earth minerals, usually in combination with cerium and other rare earth elements. According to the periodic table, lanthanum belongs to the group 3 element and is a lanthanide. It is one of the most important members in the rare earth family that can be found in combination with other rare earth elements such as cerium.

The element lanthanum consists of 57 electrons with the electronic configuration $1s^2 2s^2 2p^6 3s^2 3p^6 3d^{10} 4s^2 4p^6 4d^{10}$ $5s^2 5p^6 5d^1 6s^2$ which can also be written more compactly as [Xe] $5d^1 6s^2$. Therefore, the atoms has three valence electrons outside the noble gas core, one occupying the 5d and two the 6s subshells forming a +3 oxidation state. The electronic structure of lanthanum determines its physical properties. In this regard, the 4f states play an important role due to its effect on the low melting point and superconducting transition temperature and as has been studied by Smith et al. [1] using an electron excited X-ray appearance potential spectrum (EXAPS). It has since been known that the 4f states in the rare earth elements are found to be significantly higher (e.g., up to 5 eV) in the solid state than in the free atomic state. Nevertheless, the extensive overlap between the 4d and 4f subshells, which is dominated by multiplet splitting, makes it unsuitable for the determination of any single-particle energy level; therefore, other methods such as X-ray-excited electron appearance potential spectroscopy (XEAPS) are used to study its band structure, especially the 4f states of La have been performed by Kanski et al. [2]. Some important physical properties of La are presented in **Table 1**.

There are many applications of lanthanum; its ability as a catalyst is among these. In fact, La can be used as additives to improve the performance of other catalysts. In addition, La can also be applied as additives in glass, carbon lighting for studio lighting and projection, ignition element in lighters and torches, electron cathode, and scintillators [3]. Recently, interest in lanthanum as a dopant or an additive in ferroelectric thin film has increased due to its ability to significantly modify the optical and structural properties of its host material. Ferroelectric materials such as barium titanate ($BaTiO_{3)}$), lead titanate ($PbTiO_3$, lead zirconate ($PbZrO_3$), barium strontium titanate (BST), lithium tantalate ($LiTaO_3$), and lithium niobate ($LiNbO_3$) have many interesting applications in modern day thin film technology, such as photovoltaic thin films, color sensors, and thin film-based light emitting diodes (TFLED). Barium titanate, for example, is one of the most common ferroelectric materials, and it is used as a capacitor and ferroelectric memory due to its excellent dielectric and ferroelectric properties [4].

Physical properties	Value
Crystal structure	Double hexagonal close packed
Electronic configuration	[Xe]$5d^1 6s^2$
Atomic radius	187 pm
Ionization energy (1st)	538 kJ/mol
Thermal conductivity	13.4 W/(m K)
Magnetic property	Paramagnetic
Density near room temperature (solid)	6.16 g/cm^3
Density at melting point (liquid)	5.94 g/cm^3
Melting point	920°C
Boiling point	3464°C
Molar heat capacity	27.1 J/(mol K)

Table 1. Some physical properties of lanthanum.

http://dx.doi.org/10.5772/intechopen.69029

Ferroelectric materials are known for their ability of spontaneous electric polarization, which can be readily reversed using an external electrical field. Ferroelectricity is a result of the electric dipole moments parallel ordering without the presence of an external/applied electrical field. The adjacent dipoles have the tendency to align themselves parallel to each other forming domain structures with strong magnetic orientation. Many ferroelectric materials such as barium titanate ($BaTiO_3$), lead zirconate titanate (PZT), and lead lanthanum zirconate titanate (PLZT) are having the perovskite-type structure ABO_3.

Moreover, BST has an interesting physical property due to substitution of the barium or titanium ion with small ion/atomic dopant such as La—which has an atomic radius close to Sr^{2+} —may result in structure and microstructure changes. This leads to significant changes in the dielectric and ferroelectric properties of the thin film. The capability of these perovskite structures to host different sized ions in the BT lattice is remarkable and may even cause ferroelectric transition as we will show later in this work. At room temperature, pure barium titanate can be categorized as an electrical insulator. The presence of dopants in the BT lattice could cause lowering of electrical resistivity of materials due to atomic substitution and depend significantly on the concentration of the dopant itself. In some cases, addition of dopants may change the material property from insulating to semiconductor but may well reverse to insulator if a critical threshold is reached.

2. Effect of lanthanum doping on ferroelectric host material

The effects of lanthanum content on other ferroelectric materials such as transparent ferroelectric ceramics have been studied thoroughly by Falcao et al. [5]. In their work, the thermo-optical properties of (Pb, La)(Zr, Ti)O_3 or PLZT due to lanthanum addition were studied using thermal lens spectrometry, optical interferometry, and the thermal relaxation calorimetry. PLZT plays an important role in the photonic area, because they can be used in diode-pumped laser as an active medium. Using three different methods, they were able to determine the thermal diffusivity, thermal conductivity, changes in the optical path length, and temperature coefficient of the refractive index. They found that lanthanum addition in PLZT causes significant alteration of the mentioned thermo-optical property. However, no significant variation in the specific heat of PLZT as a result of La doping was observed. The highest values of thermal diffusivity, thermal conductivity at room temperature was obtained for a 10 mol% of lanthanum concentration addition, thus they claim that PLZT doped with La have many interesting laser applications, due to its very good thermo-optical properties.

More recently, the effects of La doping on $0.96[Bi1/2(Na_{0.84}\ K_{0.16})_{1/2}]_{(1-x)}La_xTiO_3$-$_{0.04}SrTiO_3$ (BNKTLa$_x$-ST) crystal structure and piezoelectric properties were investigated by Tran et al. [6], where they show using X-ray diffraction (XRD) that a phase transition from coexistence rhombohedral-tetragonal to a pseudocubic phase occurs due to lanthanum doping, namely, for $x = 0.02$, in the above-mentioned crystal structure. In addition, they found that by investigating the dielectric properties upon La addition, a ferroelectric to ergodic relaxor phase transition was observed.

The other work by Han et al. shows that La-modified bismuth titanate (BLT) can also be doped further by iron atoms, leading to large improvements in the bandgap property even

though challenges still exist due to the difficulty in creating BLT without forming a $BiFeO_3$ secondary phase [7]. To remove the secondary phase, Han et al. performed a solid reaction at various calcination temperatures (300–900°C). Furthermore, they apply X-ray diffraction and ultraviolet-visible absorption spectroscopy to investigate the structural and optical properties, respectively. The substitution of Fe atoms can decrease the optical bandgap of BLT, which opens the possibility for a tunable bandgap material.

Although in our work, we applied the chemical solution deposition (CSD) method, it is interesting to compare our result with the work of Bae et al. who present the ferroelectric properties of lanthanum-doped bismuth titanate thin films grown by a sol-gel method [8]. In their work, lanthanum-doped bismuth titanate, $Bi_{3.25}La_{0.75}Ti_3O_{12}$ (BLT), and thin films were grown on Pt(1 1 1)/Ti/SiO_2/Si (1 0 0) substrates by a sol-gel spin coating process. The substrate is then sufficiently annealing at 550–700°C to obtain crystallized thin films. Using X-ray diffraction (XRD), they were able to show that the ratio of the c-axis-oriented La-doped BLT grains significantly depends at the annealing temperature. They also claimed, based on the results, that lanthanum-doped BLT has the potential as an environmentally safe lead-free ferroelectric material, possessing remarkable ferroelectric properties.

Pure barium titanate possesses the property as an electrical insulator at room temperature. The addition of dopants can alter the electrical property of such materials, e.g., altering the energy bandgap, which opens promising application both in the field of optics and electronics. For the barium titanate case, the addition of dopants causes a decrease in the material electrical resistivity. Thus, by adding dopant concentration, one can change the electrical property of certain material from insulating to semiconductor. However, after reaching a certain critical threshold dopant levels, the semiconductor material may become an insulator again.

In the proceeding chapters, we describe the optical and structural properties of lanthanum-doped thin films that were characterized by using UV-visible spectrometer and X-ray diffraction, respectively. The functional groups and particle size were observed by using Fourier transform infrared (FTIR) spectrophotometer and particle size analyzer (PSA). The surface roughness was investigated using 3D (three-dimensional) atomic force microscopy (AFM). We start by explaining the experimental methods and preparation of the substrate as well as thin film growth.

3. Experimental methods, substrate preparation, thin film growth, and characterization techniques

Several methods exist in synthesizing the above-mentioned ferroelectric materials, such as pulsed laser deposition (PLD), metal organic solution deposition (MOSD), reactive sputtering, ion beam-assisted deposition (IBAD), and chemical solution deposition (CSD) method. In most of our work, ferroelectric thin films, e.g., barium titanate ($BaTiO_3$), lead barium strontium titanate (BST), lithium tantalate ($LiTaO_3$), and lithium niobate ($LiNbO_3$), were doped with lanthanum and using the CSD method. This method is based on deposition of chemical

http://dx.doi.org/10.5772/intechopen.69029

solution on the top of a substrate often followed by rotation at certain rotational speed using spin coating. Several advantages of using CSD are as follows: processing temperature can be relatively low, composition homogeneity is achieved, precise control of the composition, as well as large area deposition [9–11].

3.1. Preparation and characterization of BST, BGST, and BTST thin films

Barium strontium titanate ($Ba_{0.5}Sr_{0.5}TiO_3$-BST) was produced by using the chemical solution deposition (CSD) method with ultrasonic mixing of 0.160 g barium acetic + 0.131 g strontium acetic + 0.355 g titanium isopropoxide + 0.060 g gallium oxide as a precursor [9] for 2 h. By mixing barium acetate [Ba $(CH_3COO)_2$, 99%], strontium acetate [$Sr(CH_3COO)_2$, 99%], and titanium isopropoxide [$Ti(C_{12}O_4H_{28})$, 97.99%] with 2.5 ml of 2-methoxy ethanol as a solvent, a BST solution was obtained. The barium strontium titanate (BGST) thin films were fabricated also via CSD methods with ultrasonic mixing of 0.160 g barium acetic + 0.131 g strontium acetic + 0.355 g titanium isopropoxide + 0.060 g gallium oxide as a precursor in 1.25 ml 2-methoxyethanol solution for 2 h. Meanwhile, barium strontium titanate (BTST) was produced with the same method using 0.160 g barium acetic + 0.131 g strontium acetic + 0.355 g titanium isopropoxide + 0.060 g tantalum oxide as a precursor in 1.25 ml 2-methoxyethanol as solvents. The solutions were then stirred with a Branson 2210 ultrasonic stirrer for 90 min. Afterward, 10% gallium oxide–doped barium strontium titanate (BGST) and 10% tantalum oxide–doped barium strontium titanate (BTST) were prepared on a p-type Si (1 0 0) substrate using the chemical solution deposition (CSD) method with a precursor of 1.00 M. After 20 min in room temperature, the clear solution acquired a milky appearance. To produce a homogenous thin film, we use a spin coating method with a spinning speed of 3000 rpm for 30 s. After the deposition process, the thin film substrate was annealed in a furnace Model Nabertherm Type 27 at 200, 240, and 280°C (low temperature) for 1 h using oxygen gas as its atmosphere.

The surface roughness and grain size analysis of the grown thin films were described by the atomic force microscope (AFM) method at a 5000 × 5000 nm sample area. The rms surface roughness of our BGST thin films with 5000 × 5000 nm area are 0.632, 0.564, and 0.487 nm at the annealing temperature of 200, 240, and 280°C, respectively, whereas the grain size (mean diameter) were 238.4, 219.0, and 185.1 nm at annealing temperature of 200, 240, and 280°C, respectively. The increase of annealing temperature from 200 to 280°C resulted in a decrease of the rms roughness and grain size.

3.2. Preparation and characterization of BSLT thin films

BST doped by lanthanum oxide La_2O_3 or in short, BSLT was obtained by mixing solutions of [$Ba(CH_3COO)_2$, 9%], strontium acetate [$Sr(CH_3COOH)_2$, 99%], titanium isopropoxide [$Ti(C_{12}O_4H_{28})$, 99%], lanthanum oxide [(La_2O_3), 99%], and ethylene glycol as a solvent. The molar fraction of Ba was chosen as 0.55, while the molar fraction of Sr at 0.45 mol/l with 1.25 ml of ethylene glycol solvent. The composition and mass of each solvent were determined using the stoichiometric calculations:

$$0.55\,Ba\left(CH_3COO\right)_2 + 0.45Sr\left(CH_3COO\right)_2 + Ti\left(C_{12}O_4H_{28}\right) + 22O_2 \rightarrow Ba_{0.55}Sr_{0.45}TiO_3 + 17H_2O + 16CO_2 \quad (1)$$

Meanwhile, barium acetate, strontium acetate, and titanium isopropoxide were obtained by mixing ethylene glycol solvent and vibrated for 1 h using a Branson ultrasonic 2210. Furthermore, using the same method, 6% dopant lanthanum oxide was added and vibrated for 30 min. From the mixing process, we obtained BSLT.

To produce BSLT with 6% doping, a Si (1 1 1) type-p which had been cut with area 1 cm^2 was grown using a spin coating technique at 3000 rpm for 30 s. The next process was optimization of the film by annealing at 850°C for 15 h with a heating rate of 2°C/min using furnace VulcanTM 3-13 and dropped in temperature with the same rate to return to room temperature for 20 min. Afterward, the mass of the sample was weighed. The thin films' thicknesses were determined by the volumetric method.

The optical properties of BSLT were characterized using a Vis-NIR spectrophotometer to see the absorption spectra of thin films in large area waves (380–900 nm), then the value of energy gap can be determined with a Tauc plot and the refractive index, n with

$$n = \frac{1+\sqrt{R}}{1-\sqrt{R}} \quad (2)$$

where R is the reflectance.

The model of crystal structure of the films that has been made was characterized using X-ray diffraction (XRD), and ICDD database was used to match the diffraction peaks.

3.3. Preparation and characterization of $LiNbO_3$ thin films

$LiNbO_3$ thin films were produced in two stages [10]: in the first stage, the substrate was prepared by cutting the p-type Si (1 0 0) waver with a surface area of 8 × 8 mm then cleaned by aqua bidest and dried. In the second stage, the $LiNbO_3$ powder (precursor) was produced. The method and thin film preparation of lithium niobate were analogous with the previous BST, BGST, and BTST sample, namely, using CSD, so we will not repeat the description in length here. We used three prepared precursors, namely, undoped precursor, 5% lanthanum-doped precursor, and 10% lanthanum-doped precursor. The precursors were obtained by mixing $LiCH_3COO$ powder, Nb_2O_5, with lanthanum, and then dissolve the mixture in 2.5 ml 2-methoxy methanol. The mixing process was conducted using an ultrasonic of Branson 2210 for 90 min and then deposited on the substrate by using a spin coating method at a speed of 3000 rpm two times. The next step was annealing process using the furnace of Vulcan™3–130. The annealing process for each substrate was started from room temperature with the increasing rate of 1.7°C/min to temperature of 550°C and then held constantly for 8 h before cooled until room temperature.

The optical properties of thin films were characterized by using USB 2000 spectrometer, and their crystal structures were observed using XRD-GBC EMMA. The functional groups and particle size were characterized by using FTIR and PSA, respectively.

http://dx.doi.org/10.5772/intechopen.69029

3.4. Preparation and characterization of $LiTaO_3$ thin films

The preparation of $LiTaO_3$ thin films was performed first by cutting the (0 0 1) Si substrate with a size of 8 × 8 mm. Then, the substrates were cleaned using aqua bidest and dried. In this case, three $LiTaO_3$ solutions were prepared as in our previous work using the CSD (chemical solution deposition) method [11]. The first solution was prepared by mixing 0.1650 g of $LiCH_3COO$ and 0.5524 g of Ta_2O_5, which were soluble in 2.5 ml of 2-methoxy methanol. For the La-doped substrate, the second solution was prepared by mixing 0.1650 g of $LiCH_3COO$ and 0.5524 g of Ta_2O_5 which were soluble in 2-methoxy methanol to become $LiTaO_3$ 2.5 ml with the addition of 0.0295 g of La_2O_3 as a dopant. The obtained product is a 5% lanthanum-doped $LiTaO_3$ solution. Afterward, the third solution was prepared by mixing 0.1650 g of $LiCH_3COO$ and 0.5524 g of Ta_2O_5 which were soluble in 2.5 ml of 2-methoxy methanol with the addition of 0.0590 g of La_2O_3. The obtained product is a 10% lanthanum-doped $LiTaO_3$ solution.

The three solutions then underwent sonication process for 90 min using a Branson 2510 instrument. The solutions were then dropped toward the substrate's surface placed on a spin coating rotator with a rotation speed of 3000 rpm, conducted twice. The remaining solutions were then dried at 80°C for 24 h and then characterized using FTIR and PSA. The dropped substrates were then annealed using a furnace with an increasing rate of temperature at 1.7°C/min, started from room temperature until it reaches 550°C and held constantly for 12.5 h, and then cooled down to room temperature. The formed thin films were characterized using XRD and optical ocean USB 2000 [11].

4. Results and discussion

4.1. La-doped BST thin films

Before we explain the effect of lanthanum on barium strontium titanate (BST), we first describe our earlier works regarding the effect of the addition of nonrare earth-dopant BST because one can compare the results to similar treatment of substrates with lanthanum dopant [9].

Gallium oxide-doped barium strontium titanate and tantalum oxide-doped barium titanate are of immense interest, particularly as a ferroelectric solar cell (FSC). The roughness and grain size properties of the BST grown films, which were already doped by gallium oxide and tantalum oxide, were measured at various annealing temperature. We found that the roughness and grain size properties of the material can be tailored by varying the concentration of the dopant and annealing temperature. This opens the possibility to optimize FSC performance by varying the doping concentration and annealing temperature. We also performed 3D atomic force microscopy (AFM) imaging to observe the effect of dopant addition on the surface roughness, and the result is depicted in **Figure 1**.

The figure clearly indicates an increase in peak roughness when gallium oxide is added, resulting in BGST but shows smooth mixing roughness for BTST. Specifically, the average surface roughness for the BST thin films were 10.50, 0.6324, and 0.2202 nm at annealing temperature

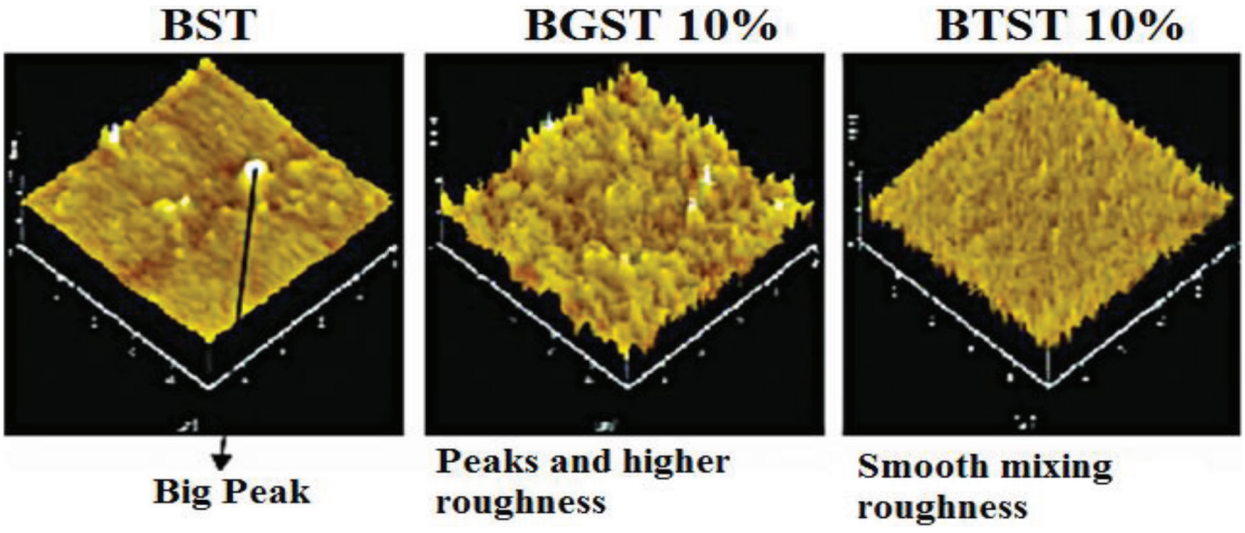

Figure 1. The three-dimensional analysis using the AFM method at 280°C of a 5000 × 5000 nm substrate area for BST, BGST, and BTST thin films [9].

of 200, 240, and 280°C, respectively, whereas the grain sizes (mean diameter) were 1.046, 238.4, and 141.3 nm, respectively. Meanwhile, the average surface roughness for BGST thin films were 0.632, 0.564, and 0.487 nm at annealing temperature of 200, 240, and 280°C, respectively, whereas the grain sizes (mean diameter) were 238.4, 219.0, and 185.1 nm, respectively. The average surface roughness for BTST thin films were 1.087, 0.4870, and 0.2317 nm at temperature 200, 240, 280°C, respectively, whereas the grain size (mean diameter) are 158.7, 291.1, and 396.7 nm, respectively [9]. Thus, we found that addition of dopants significantly alters the surface roughness and grain size, and a similar feature is expected for rare-earth, e.g., lanthanum oxide (La_2O_3) dopant on thin films.

The optical and structural effects of lanthanum oxide (La_2O_3) dopant on ferroelectric barium strontium titanate (BST) thin film were performed in our research. As expected from our previous work [9], we observe a decrease in the lattice parameter of La-doped BST thin films (BSLT) compared to nondoped thin films which were 3.936 and 3.949 Å, respectively. The reason for this decrease is due to the insertion of La atoms as substitutes in the BST lattice. We attribute the process more specifically as follows: the element lanthanum which has a radius of 1.15 Å replaces one Sr^{2+} ion in the BST structure which has radius of 1.13 Å and not the Ba^{2+} and Ti^{4+} ions which have radii of 1.35 and 0.68 Å, respectively. This preference is due to the close similarity of their atomic radii. Meanwhile, an electrostatic imbalance occurs which we attribute to an excess La^{3+} proton, which replaces one of other Sr^{2+} ions, resulting in a repulsive force with other Sr^{2+} ions in the crystal structure.

In addition, the lanthanum dopant significantly decreases the absorbance value, which is shown in **Figure 2**. This decrease in absorbance is due to the addition of La and can be attributed to the substation of La on the Sr ion which in turn changes the eigen energy level of the BSLT thin film. As shown in **Figure 3**, the insertion of La in BST increases the bandgap of the system. The result shows that the energy gap for pure BST was 1.99 and 2.67 eV for a 6% La-doped BST. The energy gap was obtained using [12]

http://dx.doi.org/10.5772/intechopen.69029

$$\left(\frac{\alpha hc}{\lambda}\right)^2 = \text{Cons.}\left(\frac{hc}{\lambda} - E_g\right) \tag{3}$$

where α is the absorption coefficient, (hc) is the incident photon energy, and E_g is the band-gap energy. The energy gap can be obtained via linear plotting $\left(\frac{\alpha hc}{\lambda}\right)$ versus E_g. As shown in **Figure 2**, both pure BST and BSLT thin films have good absorption in the range of 400–700 nm which is in the visible light spectrum. Therefore, it is not surprising that we find a decrease in the absorbance spectrum since the electrons are now unable to absorb photons with energy less than the bandgap energy as was possible for undoped BST (smaller energy gap). Again, *ab initio* quantum mechanical calculation is necessary to investigate the full-band structure of BSLT, which is beyond the scope of this work.

Furthermore, we measured and found that the addition of lanthanum oxide will increase the refractive index and energy gap of the semiconductor thin films, which is depicted in **Table 2**. These numbers were obtained using Eq. (2). This indicates that the electrons are harder to be displaced from the valence band to the conduction band.

The crystal structure of BST films was characterized using XRD. **Figure 4** shows that diffraction peaks on each sample were in accordance with the peaks of BST on JCPDF data number 39-1395. The peaks of BST were obtained at the angle of 2θ: 22.49, 45.58, 66.98, and 76.22° corresponding to Miller planes of (1 0 0), (2 0 0), (2 2 0), and (3 1 0). The addition of lanthanum on BST films results in a decrease of the diffraction peaks but also contributes to the occurrences of new peaks at a diffraction angle of 2θ: 32.09 and 76.22°, corresponding to Miller

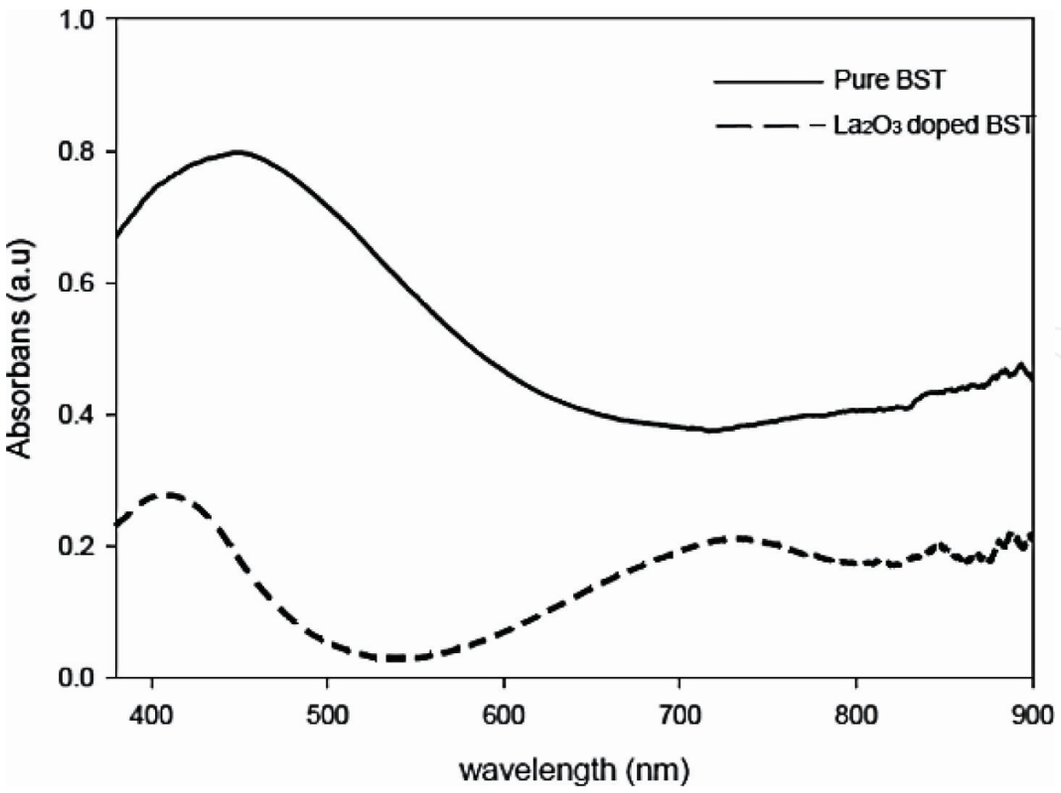

Figure 2. Absorbance curve for BST and BSLT thin films.

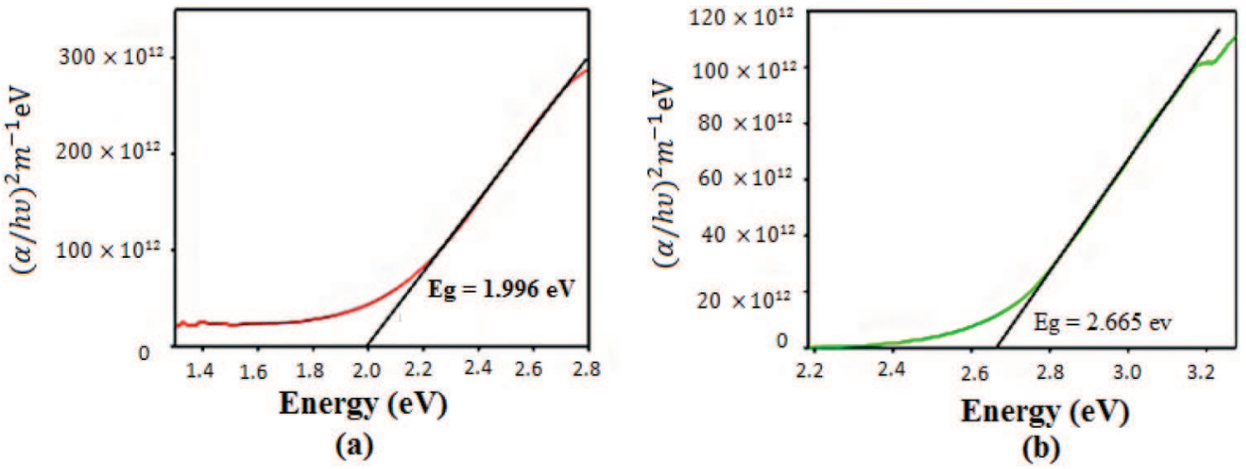

Figure 3. Energy gap of (a) undoped BST and (b) 6% La-doped BST thin films.

Film	Refractive index	Energy (eV)
BST 0%	4.386	1.996
BSLT 6%	13.118	2.665

Table 2. The refractive index and energy for BST and BSLT 6%.

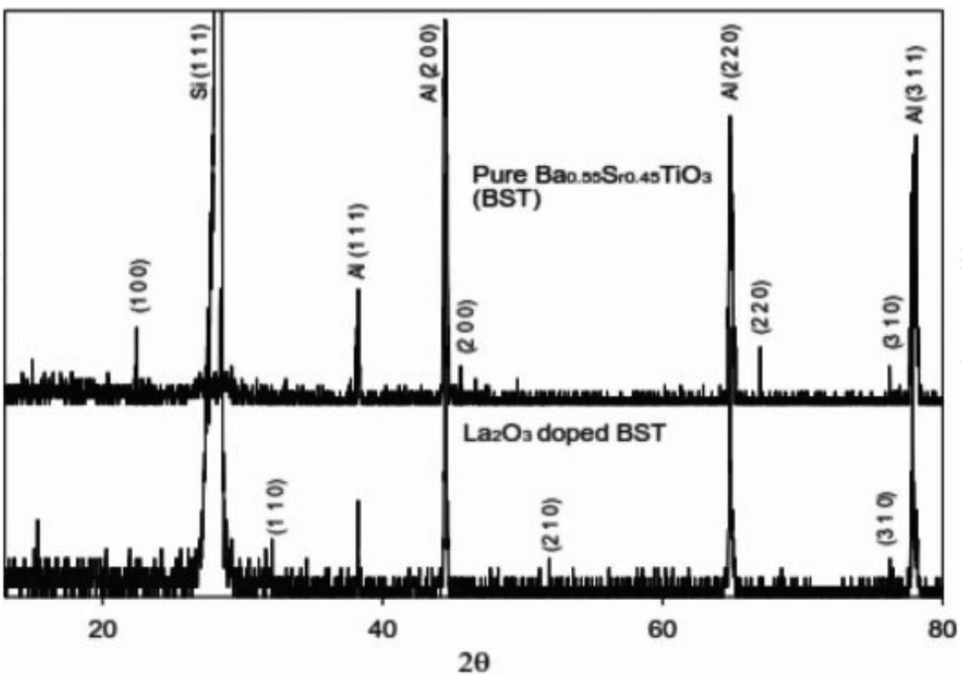

Figure 4. XRD pattern of BST and BST doped La_2O_3 (BSLT) thin films.

http://dx.doi.org/10.5772/intechopen.69029

planes of (1 1 0) and (2 1 0). The result shows that addition of lanthanum oxide affects the lattice parameter value of BST, where the symmetry of BSLT is cubic.

Interestingly, this decrease-occurrences diffraction pattern is also obtained from the beforementioned work of Tran et al. in **Figure 1** of Ref. [6]. Specifically, their XRD pattern shows that the undoped BNKT-ST ceramic sintered at 1175°C for 2 h has a morphotropic phase boundary mixture of tetragonal and rhombohedral symmetry. However, upon addition of lanthanum, some of the peaks gradually decreased, indicating a phase transition from coexistence of rhombohedral and tetragonal phases to a pseudocubic phase. They suggest that La successfully diffused into the BNKT-ST lattice and in turn forming a homogeneous solid solution which seems to be the same as in our case.

The lattice parameters of BST and BSLT were obtained using the Rietveld method where we obtained the values $a = b = c$ and $\alpha = \beta = \gamma = 90°$ indicating that BST and BSLT films have cubic Bravais lattice. Therefore, the films can easily be grown on a diamond cubic silicon substrate due to their similar crystal structure [13].

4.2. La doped lithium niobate thin films

In addition to BST, we have also recently investigated the optical and structural properties of lanthanum-doped lithium niobate ($LiNbO_3$) thin films. Lithium niobate has a trigonal crystal system. Such a system lacks an inversion symmetry; hence, surface characterization using second harmonic nonlinear spectroscopic methods is not suggested due to radiation from within the bulk. However, some nonlinear effects do occur such as the Pockels effect can be observed. Lithium niobate possesses ferroelectrical behavior and is transparent when shined by visible light.

Figure 5 shows the relationship between reflectance and wavelength of lanthanum-doped $LiNbO_3$ thin films. It can be inferred that the dopant concentration affects the reflectance intensity, e.g., 5% lanthanum-doped films increase the reflectance intensity, but conversely, 10% lanthanum-doped thin films decrease the reflectance intensity. The reason why the reflectance intensity decreases for the 10% lanthanum doping is due to the increase in the constituent atoms, which in turn increases the collision between light particle and atoms; therefore, it becomes more difficult for the light to pass through. The less transparent the film leads to higher absorbance value and damping constant and thus the lower the transmittance value [14, 15].

The optical properties of lithium niobate have been determined by Mamoun et al. using the generalized gradient approximation (GGA) method with indirect bandgaps. They found that the energy bandgaps of $LiNbO_3$ using the GGA method were 3.32 and 3.61 eV [16]. **Figure 6** shows that the energy gap for undoped, 5, and 10% lanthanum-doped thin films were 2.75, 2.80, and 2.43 eV, respectively showing that the addition of lanthanum does not produce a consistent increase or decrease. As earlier, the energy gaps were determined using Tauc plot analysis. wRemarkably, the small increase for small La-doping concentration and decrease for higher La-doping concentration is in agreement with the results shown in **Figure 10** of Ref. [17]. The researchers argue that the observed lowering of energy gap with La doping could be due to

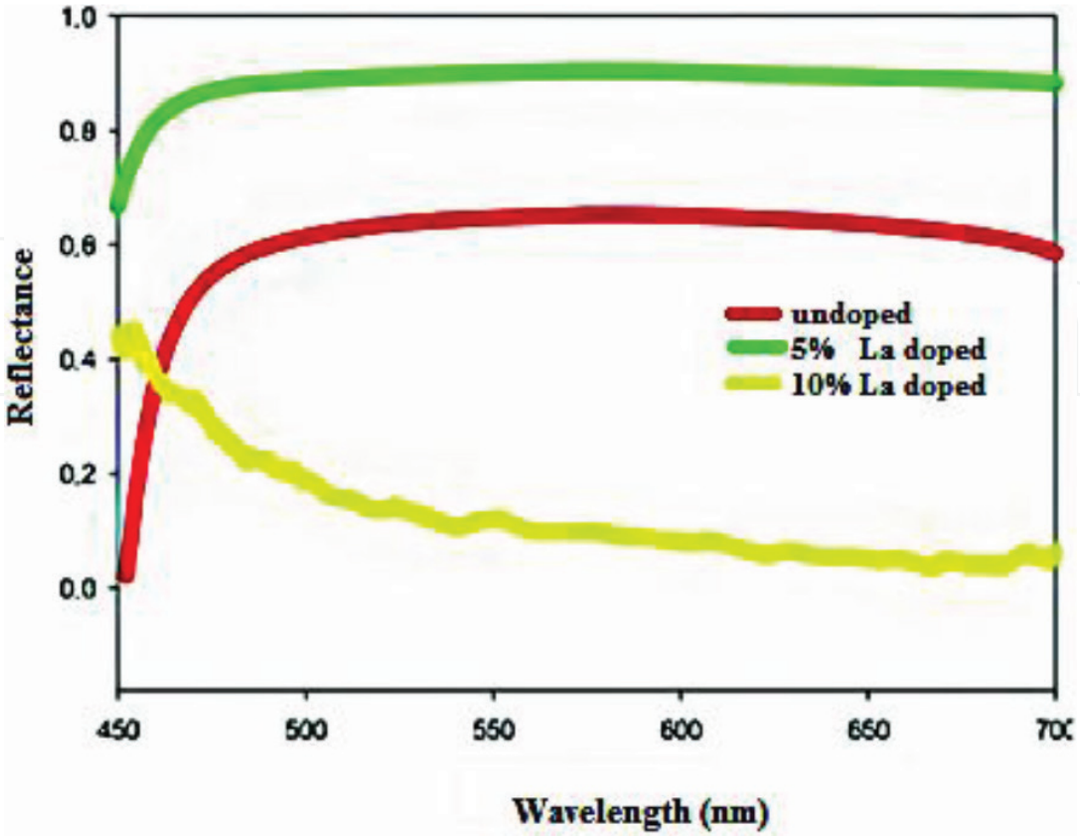

Figure 5. Reflectance of undoped and doped $LiNbO_3$ thin films at several wavelength [10].

the combined effect of increased grain size and improved crystallinity with increase in dopant concentration [17]. From the quantum mechanical point of view, the increase in the absorbance for a higher doping concentrated can be attributed to the decrease in the bandgap due to overlapping energy levels which could in principle be calculated using Density Functional Theory (DFT) or other *ab initio* methods. Up to now, the bandgap decreases—more light with less energy can be absorbed resulting in an increase in absorption. The absorption is high in the UV region and low in the IR region.

Furthermore, we also performed FTIR spectroscopic measurements on lanthanum-doped $LiNbO_3$ thin films to investigate the presence of functional groups: O-H, N-H, C=C, C-O, C-H, and hexagonal crystal symmetry. The result is present in **Figure 7**. A higher dopant concentration leads to a smaller lattice parameter. It was found that the particle sizes of undoped, 5, and 10% lanthanum doped films were 1230.59, 977.5, and 741.51 nm, respectively, thus showing a consistent decrease in the lattice parameter smaller than that of lithium niobate. The decrease in crystal size is also influenced by the radius of its constituent ions. Ionic radii of Li^+, Nb^{5+}, and La^{3+} were 0.90, 0.78, and 1.172 Å, respectively. We attribute this decrease to the following: the ionic radius of La^{3+} is closer to that of Li^+; therefore, La^{3+} can replace the positions of Li^+ in the crystal structure. Because the replaced dopant size is smaller, it leads to an overall decrease in the crystal size of doped $LiNbO_3$.

Figure 8 shows the XRD pattern of $LiNbO_3$ thin films, which are deposited on the p-type silicon (1 0 0) substrate after the annealing process at 550°C. The data were collected with interval

http://dx.doi.org/10.5772/intechopen.69029

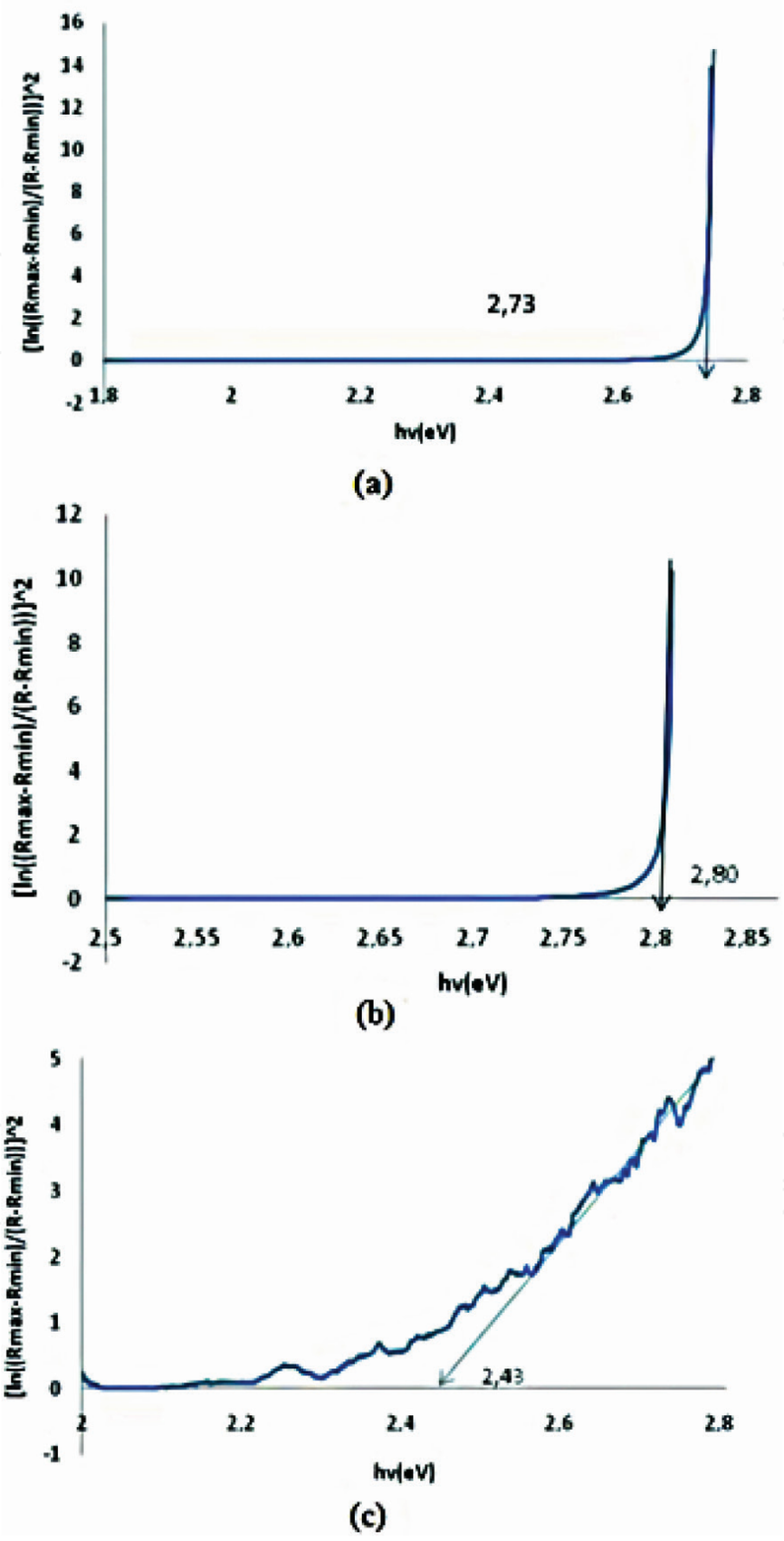

Figure 6. Tauc plot method to determine the energy gap for (a) undoped (b) 5% lanthanum doped, and (c) 10% lanthanum-doped $LiNbO_3$ thin films [10].

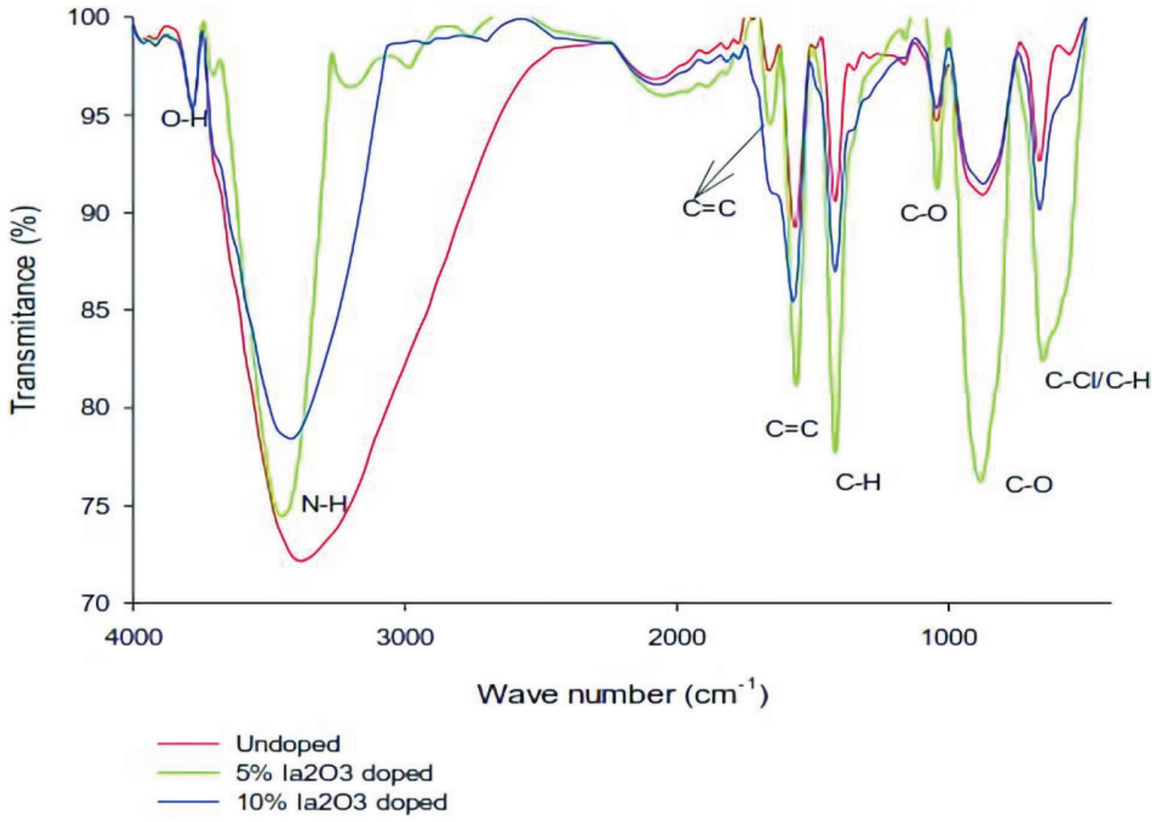

Figure 7. The FTIR spectra of $LiNbO_3$ thin films [10].

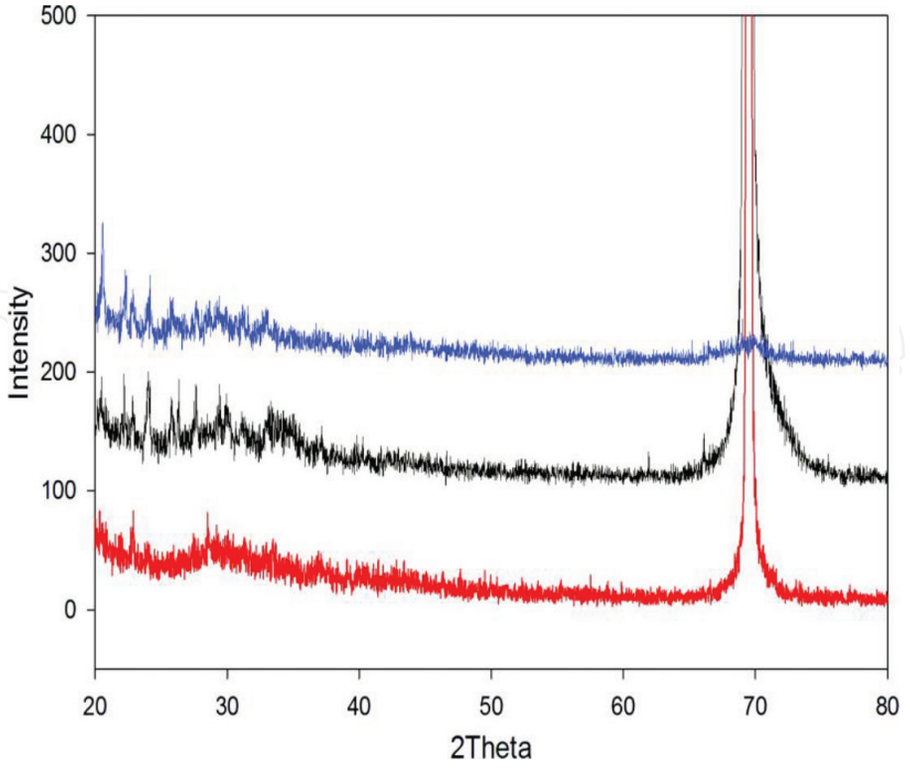

Figure 8. The XRD pattern of $LiNbO_3$ thin films [10].

http://dx.doi.org/10.5772/intechopen.69029

0.02° in the range of 10–80°C. Compared to JCPDS (Joint committee on powder diffraction standard) data, the peaks of $LiNbO_3$ are formed in the (h k l) of (0 1 2) and (1 0 4). In addition, the peaks are in the h k l of (1 0 0), (0 0 2), and (1 0 1) for thin films doped with lanthanum. The lanthanum dopant also affects the quality of $LiNbO_3$ crystal, addition of 10% dopant concentration is followed by a decrease in the crystal intensity peak at a Miller indices (hkl) of (0 1 2), while 5% dopant (blue) results in the increases the intensity peak. However, a contrary result is obtained for the 10% La dopant. The lattice parameters of $LiNbO_3$ and lanthanum were calculated using the Cohen method [13]. From the calculation and database, it is known that lattice parameter of lanthanum is smaller than that of lithium niobate, thus it can be said that the dopant addition will decrease the lattice parameter of $LiNbO_3$.

Very recently, we also performed 3D AFM imaging similar to the previous work on doped BST to investigate the surface roughness. As expected, increase in La doping results in a surface roughening as depicted in **Figure 9**. We attribute this roughening due to local strain effects due to substitution atoms, which will affect the growth kinetic process. However, an increase of dopants up to an optimal value may well lower the roughness if the spatial variations of the local strain can become less. Further work is underway to understand the fundamental physical process regarding this roughening, and the result will be reported elsewhere.

4.3. La-doped lithium tantalite thin films

In the following section, we report the effect of La doping on lithium tantalite ($LiTaO_3$) thin films, which is based on our previous work [11]. $LiTaO_3$ is one of the widely used optoelectronics materials due to its ferroelectric, piezoelectric, and pyroelectric properties. It is also an attractive material for integrated-optic applications due to its nonlinear optical properties, large electroptic and piezoelectric coefficient and its superior resistance to laser-induced optical damage. Thus, $LiTaO_3$ is a ferroelectric crystal that undergoes high Curie temperature of 608°C, and it also has high melting temperature at 1650°C [15]. **Figure 10** shows that the energy gaps of undoped, 5% La doped, and 10% La-doped thin films are 2.550, 2.020, and 2.199 eV, respectively.

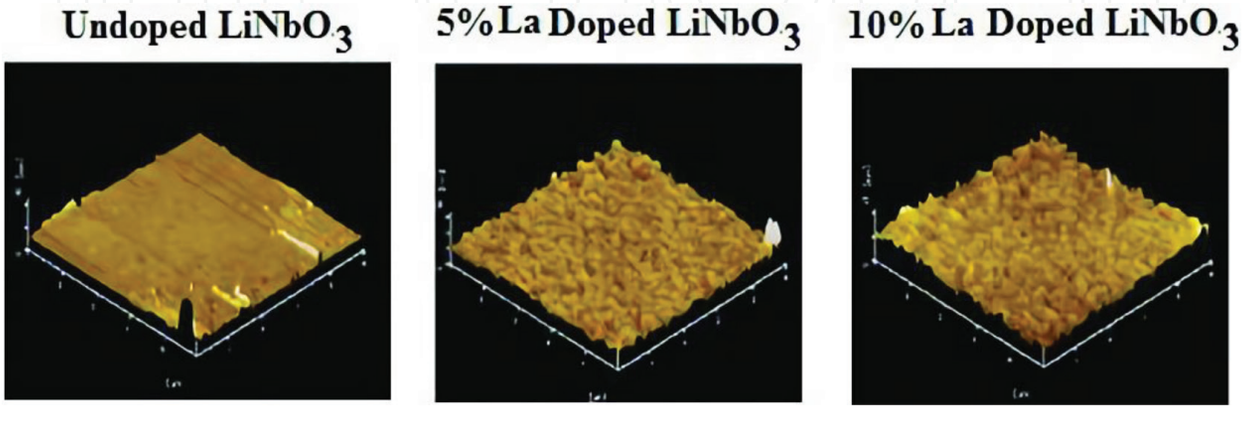

Figure 9. 3D AFM surface roughness of undoped LiNbO, 5% La doped LiNbO, and 10% LiNbO [10].

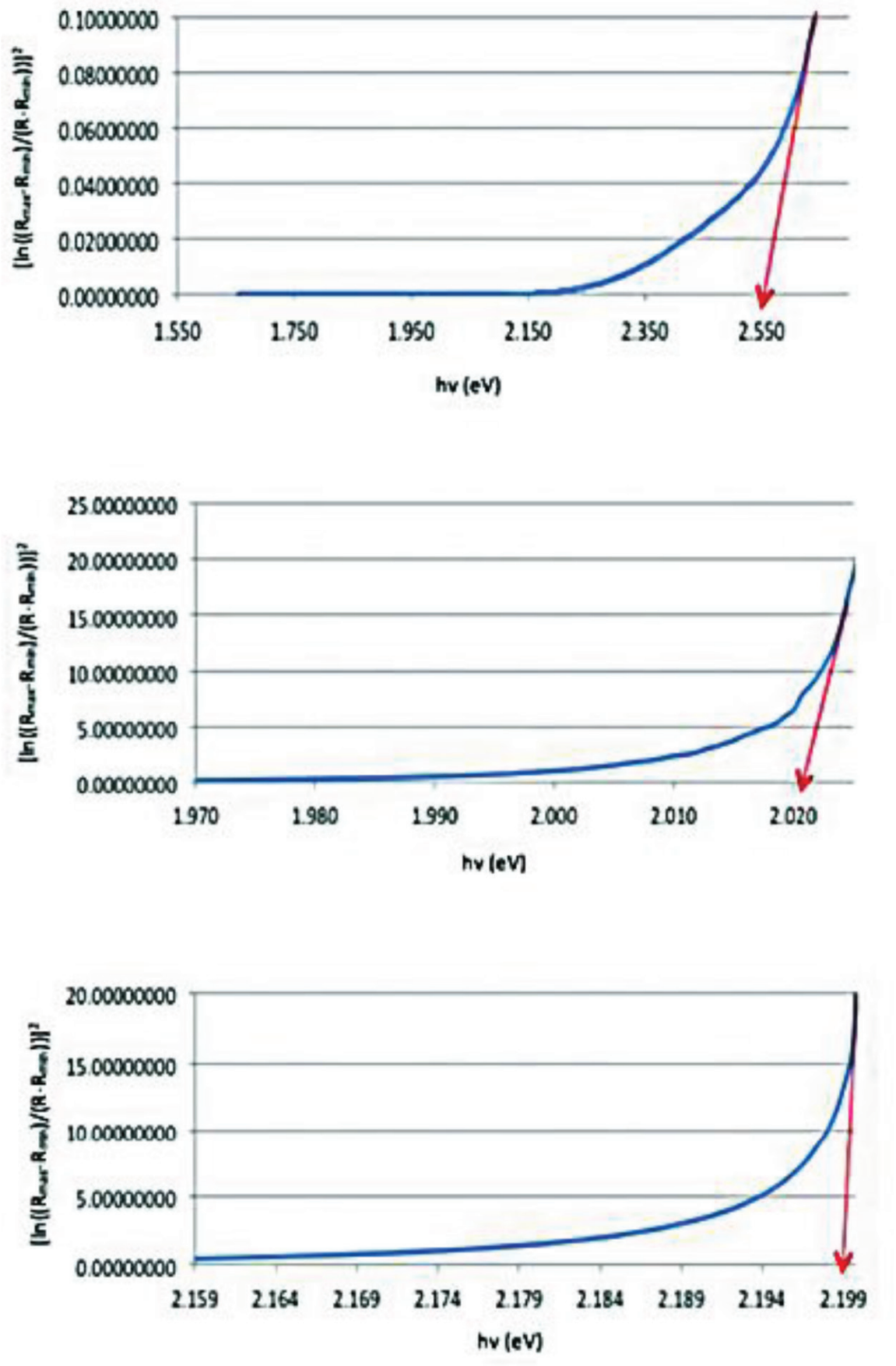

Figure 10. Energy gap of (a) undoped, (b) 5% doped, and (c) 10% doped $LiTaO_3$ thin films [11].

http://dx.doi.org/10.5772/intechopen.69029

It can be concluded that the higher dopant concentration leads to the lower energy gap, which means the electron will be easier to move from the valence band area into the conduction band.

The energy gap in lithium tantalite is smaller than that obtained in lithium niobate. In this research, the overall values of energy gap of thin films from silicon substrate are in the range of 2.0–3.45 eV for all concentrations. *Ab initio* quantum mechanical calculations focusing on overlapping of eigen energy levels between the La upon Na and Ta energy bands should be performed to investigate the energy gap more comprehensively, but it is beyond the scope of our work.

It is well known that the energy gap of pure silicon is typically 0.7 eV. Silicon itself is usually used as a semiconductor material and has been applied on many electronic devices due to its unique energy gap. We found that there is energy gap increase for a La dopant concentration between 5 and 10%. This is in accordance with the other researcher-related work, which also found the energy gap to increase after dopant addition [18, 19]. Indeed, this result is known as the Burstein-Moss effect, which is the increase in the bandgap value of a thin film–doped semiconductor due to electrons in the conduction band shifting the Fermi level and causes an increasing bandgap [20]. The phenomenon of which the apparent bandgap of a semiconductor is increased as the absorption edge is pushed to higher energies is due to of all states that lie close to the conduction band being already populated.

Figure 11 shows the XRD pattern of $LiTaO_3$ thin films with the p-type Si (1 0 0) substrate after annealing at 550°C. The data were obtained within an interval of 0.02° in the range of 20–80°C. These three patterns show a peak at $2\theta = 70°$ corresponding to the silicon substrate. The XRD pattern shows that $LiTaO_3$ thin films have both crystalline and amorphous

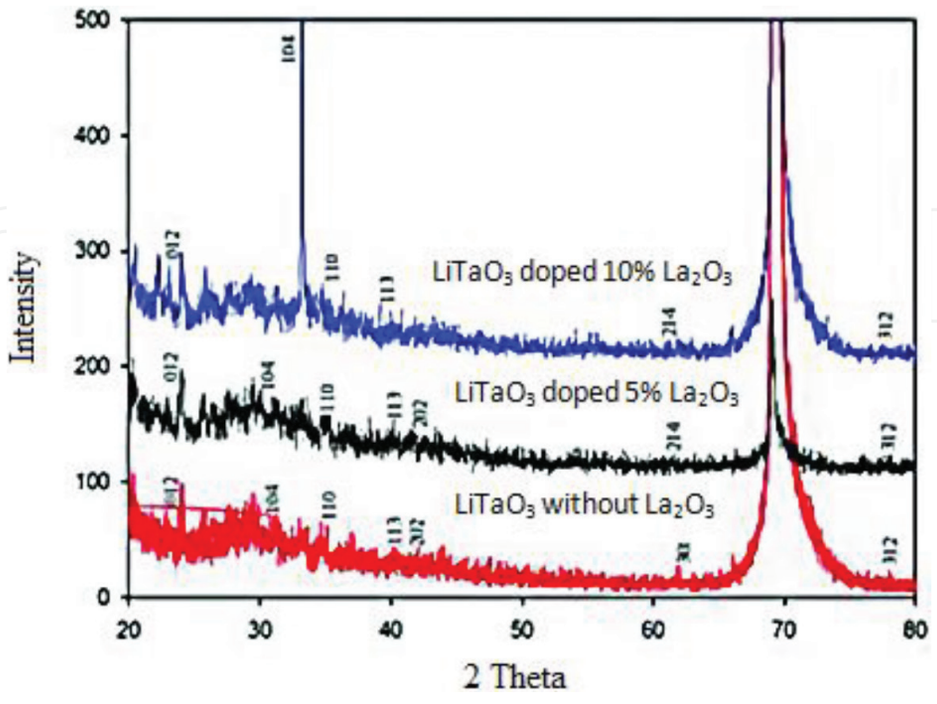

Figure 11. The XRD pattern of $LiTaO_3$ thin film with p-type Si (1 0 0) substrate after annealing at 550°C. Li^+ in the crystal structure [11].

structures. The undoped $LiTaO_3$ thin films have mixed structure with lattice parameters a = 5.13 Å and c = 13.54 Å. Meanwhile, for the 5% La-doped $LiTaO_3$ thin films, the XRD pattern shows that the structure is not significantly different compared to that of without doping albeit smaller lattice parameters: a = 4.92 Å and c = 14.19 Å. Moreover, for the 10% La_2O_3 doped $LiTaO_3$ thin films, a peak of $LiTaO_3$ with a lattice parameter of a = 5.11 Å and c = 13.30 Å is present. We also argue that the decrease in crystal size is influenced by the radii of its constituent ions.

We measure the ionic radii of Li^+, Ta^{5+}, and La^{3+} to be 0.90, 0.78, and 1.172 Å, respectively. The ionic radius of La^{3+} is closer to that of Li+; therefore, we propose that the La^{3+} ion can occupy the positions of the La-doped $LiTaO_3$ thin films. The difference of ionic radii between dopant and replaced ion affects the formation of spinel phase. This leads to crystal size decreasing due to the existence of dopant cations in the $LiTaO_3$ structure. Furthermore, investigation of the composition using FTIR shows the existence of stretching vibration of OH group, C=C aromatic bonding, Li–O bonding, and Ta–O bonding at wave numbers of 3100–3900, 1650–1450, 1440–1420, and 610–945 cm^{-1}, respectively. The FTIR result is depicted in **Figure 12**.

The addition of 5% La-dopant significantly increases the refractive index compared to the undoped thin films. However, at a 10% La dopant, the refractive index decreases with respect to the undoped, as shown in **Figure 13**, the physical reason of this decrease is still not known to us. Further work needs to be performed to explain this result, e.g., studying the band structure effect due to dopant at various wavelengths.

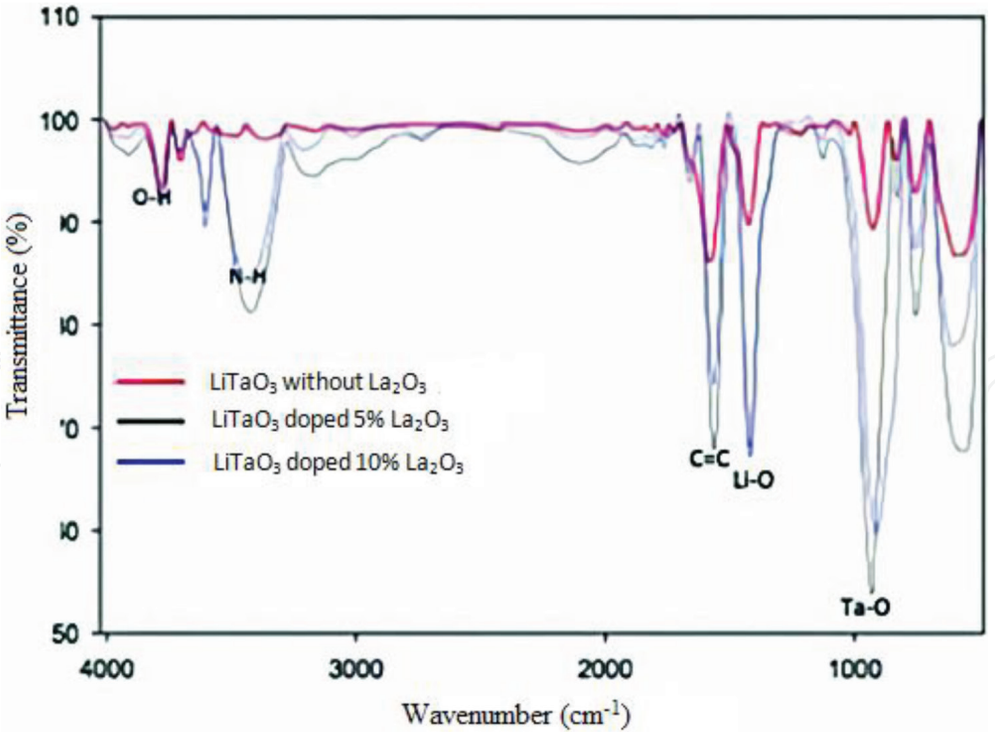

Figure 12. FTIR spectra of La doped and undoped $LiTaO_3$ [11].

http://dx.doi.org/10.5772/intechopen.69029

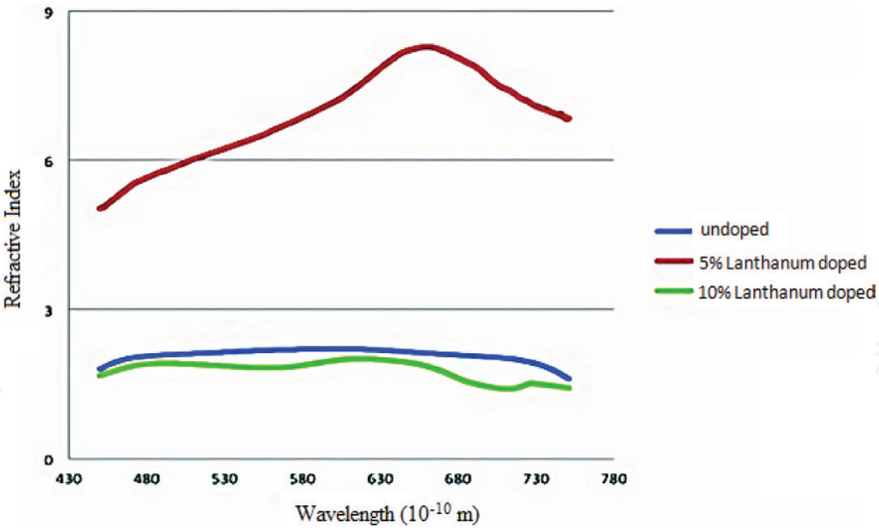

Figure 13. Refractive index variation due to La doping on $LiTaO_3$ [11].

5. Conclusion

We have showed that the effect of lanthanum doping on a ferroelectric thin film produces significant changes in its structural and optical property. The optical and structural effects of lanthanum oxide (La_2O_3) dopant on ferroelectric barium strontium titanate (BST) thin film results in a decrease in the lattice parameter of La-doped BST thin films (BSLT) compared to nondoped thin films. The addition of lanthanum oxide dopant on BST films results in a decrease of the diffraction peaks but also contributes to the occurrences of new peaks at a diffraction angle. The reason for this decrease is due to the insertion of La atoms as substitutes of Sr^{2+} in the BST lattice. This preference is due to the close similarity of their atomic radii. Meanwhile, addition of lanthanum dopant on lithium niobate thin films affects the reflectance intensity, e.g., 5% lanthanum doped increase the reflectance intensity, but conversely, 10% lanthanum-doped thin films decrease the reflectance intensity. From the quantum mechanical point of view, the increase in the absorbance for a higher doping concentrated can be attributed to the decrease in the bandgap due to overlapping energy levels, which could in principle be calculated using DFT or other *ab initio* methods. The 3D AFM imaging on La-doped lithium niobate produced similar results as for doped BST, namely, an increase in the surface roughening due to dopant. Finally, the addition of lanthanum on lithium tantalite shows the energy gap decrease of La dopant thin films compared to the undoped but increase slightly for the 10% La concentration. This is in accordance with other researcher-related work, which also found the energy gap to increase after continuous dopant addition confirming the Burstein-Moss effect. The phenomenon of which the apparent bandgap of a semiconductor is increased as the absorption edge is pushed to higher energies is due to of all states that lie close to the conduction band being already populated thus shifting up the Fermi level.

Acknowledgements

This work was funded by the International Research Collaboration and Scientific Publication under contract No. 082/SP2H/UPL/DIT.LITABMAS/II/2015 and Penelitian Institusional Institut Pertanian Bogor in 2016, Ministry of Research, Technology, and Higher Education, Republic of Indonesia.

Author details

Irzaman[1]*, Hendradi Hardhienata[1], Akhiruddin Maddu[1], Aminullah[2] and Husin Alatas[1]

*Address all correspondence to: irzaman@apps.ipb.ac.id

1 Department of Physics, Faculty of Mathematics and Natural Sciences, Bogor Agricultural University of Indonesia, Bogor, Indonesia

2 Department of Food Technology and Nutrition, Djuanda University of Indonesia, Bogor, Indonesia

References

[1] Smith RJ, Piacentini M, Lynch DW. Multiplet structure below "Threshold" in appearance-potential spectra—lanthanum $N_{4,5}$. Physical Review Letters. 1975;**34**(8):476-479

[2] Kanski J, Nilsson PO, Curelaru I. Studies of the 4f states in lanthanum by means of electron and photon excited appearance potential spectroscopy. Journal of Physics F: Metal Physics. 1976;**6**:1073-1077

[3] Moore RJ. Lanthanum: Compounds, Production and Applications, Chemistry Research and Applications. New York: Nova Science Publishers; 2011. pp. 349-363

[4] Cai W, Fu C, Gao J, Zhao C. Dielectric properties and microstructure of Mg doped barium titanate ceramics. Advances in Applied Ceramics. 2011;**110**(3):181-185

[5] Falcao EA, Eiras JA, Garcia D, Santos IA, Medina AN, Baesso ML, Catunda T, Guo R, Bhalla AS. Effects of lanthanum content on the thermo-optical properties of (Pb,La)$(Zr,Ti)O_3$. Ferroelectrics. 2016;**494**(1):33-42

[6] Tran VDN, Ullah A, Dinh TH, et al. Effect of lanthanum doping on ferroelectric and strain properties of $0.96Bi_{1/2}(Na_{0.84}K_{0.16})_{1/2}TiO_3$-$0.04SrTiO_3$ lead-free ceramics. Journal of Electronic Materials. 2016;**45**:2639-2643

[7] Han JY, Bark CW. Tunable band gap of iron-doped lanthanum-modified bismuth titanate synthesized by using the thermal decomposition of a secondary phase. Journal of the Korean Physical Society. 2015;**66**:1371-1375

[8] Bae J, Kimb SS, Choib EK, Songc TK, Kimb W-J, Lee Y-I. Ferroelectric properties of lanthanum-doped bismuth titanate thin films grown by a sol–gel method. Thin Solid Films. 2005;**472**(1-2):90-94

[9] Irzaman, Darmasetiawan H, Hardhienata H, Hikam M, Arifin P, Jusoh, S. Taking SN, Jamal Z, Idris MA. Electrical properties of photodiode $Ba_{0.25}Sr_{0.75}TiO_3$ (BST) thin film doped with ferric oxide on p-type Si (1 0 0) substrate using chemical solution deposition method. Atom Indonesia. 2009;**35**(1):133-138

[10] Irzaman, Sitompul H, Masitoh, Misbakhusshudur M, Mursyidah. Optical and structural properties of lanthanum doped lithium niobate thin films. Ferroelectrics. 2016;**502**(1):9-18

[11] Irzaman, Pebriyanto Y, Apipah ER, Noor I, Alkadri A. Characterization of optical and structural of lanthanum doped $LiTaO_3$ thin films. Integrated Ferroelectrics. 2015;**167**(1): 137-145

[12] Itskovsky MA. Kinetics of ferroelectric phase transition: Nonlinear pyroelectric effect and ferroelectric solar cell. Japanese Journal of Applied Physics. 1999;**38**(8):4812-4817

[13] Wang SY, Cheng BL, Wang C, Dai SY, Lu HB, Zhou YL, Chen ZH, Yang GZ. Raman spectroscopy studies of Ce-doping effects on $Ba_{0.5}Sr_{0.5}TiO_3$ thin films. Applied Physics Letters. 2004;**84**:4116

[14] Shandilya S, Sreenivasa K, Katiyarb RS, Gupta V. Structural and optical studies on texture $LiNbO_3$ thin film on (0 0 0 1) sapphire. Indian Journal of Engineering & Materials Science. 2008;**15**:355-357

[15] Irzaman, Syafutra H, Arif A, Alatas H, Hilaluddin MN, Kurniawan A, Iskandar J, Dahrul M, Ismangil A, Yosman D, Aminullah, Prasetyo LB, Yusuf A, Kadri TM. Formation of solar cells based on Ba0.5 Sr0.5 TiO_3 (BST) ferroelectric thick film. 5th Nanoscience and Nanotechnology Symposium (NNS2013). AIP Conference Proceedings. 2014;**1586**:24-34.

[16] Mamoun S, Merad AS, Guilbert L. Electronic and optical properties of lithium niobate from density functional theory. Computational Materials Science. 2013;**79**:125-131

[17] Majumder SB, Jain M, Katiyar RS. Investigations on the optical properties of sol–gel derived lanthanum doped lead titanate thin films. Thin Solid Films. 2002;**402**:90-98

[18] Ahmed AS, Muhamed Shafeeq M, Singla ML, Tabassum S, Naqvi AH, Azam A. Band gap narrowing and fluorescence properties of nickel doped SnO_2 nanoparticles. Journal of Luminescence. 2011;**131**:1-6

[19] Chakraborty M, Ghosh A, Thangavel R. Experimental and theoretical investigations of structural and optical properties of copper doped ZnO nanorods. Journal of Sol-Gel Science and Technology. 2015;**74**:756-764

[20] Manser JS, Kamat P. Band filling with free charge carriers in organometal halide perovskites. Nature Photonics. 2014;**8**(9):737-743

IntechOpen